Journal of the Chinese Society of Mechanical Engineers, Vol.47, No.3, pp 285~294 (2026)

Effects of PWHT on the Microstructure and Mechanical Properties of GTAW-Welded IS2062E350C Pressure Vessel Steel

Alok Vardhan* and Gajesh Kumar*

Keywords： IS2062E350C mild Steel, Post-weld heat treatment (PWHT), Gas tungsten arc welding (GTAW), Tensile test, Microhardness test, Impact test, Macrostructure, and microstructure analysis.

ABSTRACT

This study investigates the effects of post-weld heat treatment (PWHT) on the microstructural and mechanical properties of IS2062E350C mild steel welded using the gas tungsten arc welding (GTAW) process for pressure vessel applications. Welded joints were fabricated using ER70S6 filler wire, followed by PWHT at 600 °C for one hour. Comparative analysis was performed between as-welded and PWHT-treated samples through tensile testing, Charpy impact testing, Vickers microhardness measurement, and detailed macro- and microstructural characterization. The PWHT samples exhibited significantly improved impact toughness (42.5 J vs. 33 J), reduced microhardness in the heat-affected and weld zones, and refined grain structures, contributing to enhanced ductility and reduced brittleness. Although a marginal decrease in tensile strength was observed post-PWHT (498 MPa vs. 535 MPa), the joints remained structurally sound, with fracture occurring outside the weld zone. ImageJ-based quantitative analysis confirmed grain size refinement and increased ferrite phase fraction in PWHT-treated joints. These findings validate the role of PWHT in enhancing weld performance and reliability for pressure vessels, offering practical guidance for optimizing welding and heat treatment parameters in safety-critical applications.

INTRODUCTION

The concept of pressure vessels dates back to 1495, when Leonardo da Vinci introduced a design in Codex Madrid I, illustrating the use of pressurized air to lift heavy weights underwater (Nilsen, 2011).

Paper Received March 2025. Revised May 2025. Accepted July, 2025. Author for Correspondence: Alok Vardhan.

* *Assistant Professor, Department of Mechanical Engineering, Ajay Kumar Garg Engineering College Ghaziabad, India.*

Today, pressure vessels are indispensable across various industries, designed to safely contain fluids at pressures and temperatures significantly above atmospheric levels. Standards from the American Society of Mechanical Engineers (ASME) and the American Institute of Aeronautics and Astronautics (AIAA) govern pressure vessel design, fabrication, and maintenance to ensure operational stability and safety. A fractured pressure vessel poses risks of hazardous leaks or explosions, emphasizing the importance of strong construction and reliable joint integrity (Toudehdehghan et al., 2019).

A pressure vessel’s structural integrity is particularly critical, as it is exposed to extreme pressures and temperatures, making joint quality essential for safety and reliability. Welding is crucial in constructing pressure vessels, with gas tungsten arc welding (GTAW) commonly employed for its ability to create high-quality welds with minimal spatter and deformation, resulting in a robust and visually pleasing joint. However, the heat produced during welding can alter the properties in the heat-affected zone (HAZ) – a region adjacent to the weld where metal properties may differ from the unaffected base material. These variations can make the HAZ prone to fractures, especially in regions where microstructural and mechanical properties differ due to the uneven heat distribution during welding.

To mitigate this risk, researchers have studied various welding techniques and parameters. Extensive research has focused on the effects of welding conditions on the microstructural and mechanical properties of low-carbon and mild steels. For instance, Boumerzoug et al. (2010) examined the impact of welding on low-carbon steel’s microstructure and mechanical properties for gas storage cylinders, finding that fractures often occur in the HAZ where quenching conditions induce intergranular and transgranular fracture modes. Similarly, Elfallah (2023) explored the influence of factors like base metal thickness, welding current, and welding speed on tensile strength and hardness in GTAW-welded mild steel. Findings highlight that adjusting these parameters can enhance the overall strength and integrity of welded joints, which is critical for pressure vessels.

An effective approach to strengthening the HAZ and reducing the risk of fracture is post-weld heat treatment (PWHT). PWHT has shown to improve the mechanical properties of welded joints by reducing residual stresses, enhancing microstructural homogeneity, and increasing ductility, which is essential for materials that endure high-pressure and stress in operational environments. Research by Ahmed et al. (2019) on the durability of welds in LPG tanks supports PWHT's role in achieving consistent joint stability. Singh (2021) also demonstrated that heat treatment could modify key properties such as ductility, toughness, hardness, and tensile strength, optimizing steel's performance under demanding conditions. PWHT at 600°C is recognized as an effective treatment, especially for mild and stainless steels used in pressure vessels, as it balances hardness and impact toughness while achieving structural reliability (Khan et al., 2021).

Despite these advances, further experimental data is required to fully understand PWHT's impact on the mechanical and microstructural properties of GTAW pressure welds, particularly in pressure vessel applications. Past studies show PWHT reduces hardness and increases impact toughness in mild steel joints while slightly decreasing tensile strength to maintain ductility (Kumar et al., 2021). This balance between strength and ductility is crucial for pressure vessels, which must resist internal pressure without fracturing suddenly. Achieving this balance involves reducing brittleness while ensuring the material can withstand high-stress loads (Sadeghi et al., 2018).

This study aims to contribute to this area by examining the effects of PWHT on GTAW-welded joints made from IS2062E350C mild steel, specifically focusing on as-welded versus PWHT-treated joints. Key mechanical parameters like impact toughness, tensile strength, hardness, and microstructure were assessed through extensive testing and detailed microstructural analysis. By evaluating how PWHT modifies the HAZ, the study aims to show how achieving a more homogenous microstructure can enhance joint reliability in mild steel welds (Bhanu et al., 2022).

The insights from this study are intended to inform best practices for welding and PWHT protocols, providing data for enhancing pressure vessel joint reliability. Understanding optimal welding and PWHT conditions can help engineers design vessels that meet stringent safety and performance standards essential for high-stress applications. Ultimately, these findings aim to improve pressure vessel design and longevity, benefiting industries that rely on these critical components, including oil and gas, chemical processing, and power generation.

MATERIALS AND METHODOLOGY

Materials

This research is based on the use of IS2062E350C grade steel plate of dimensions (100mm x 150mm x 3mm) was used for making weld joint, as shown in Fig. 1(a). The mechanical properties of mild steel IS2062E350C, as specified in Table 1. The composition of the plate was analyzed using an optical emission spectrometer and is described in Table 2. The decision of utilizing this specific material was advised by evaluation of its mechanical properties and suitability for heat treatment applications (Singh, 2021). Taguchi's method provides guidance on utilizing the sheet's thickness to get better results (Elfallah, 2023). Generally, material used for constructing pressure vessel are stainless steel, low carbon steel can be used where corrosion is not a fact. IS2062E350C is a high strength (minimum yield strength of 350 MPa) low alloy steel which is renowned for its good weldability due to low carbon content, with improved toughness. It could be possible material for fabrication of general-purpose pressure vessel as it possesses similar properties to the material which are used for constructing pressure vessels. The stainless steel is costlier as compared to low alloy carbon steel because of its corrosion resistance. Mild steel weld joint with thickness of 3mm were received in normalized and tempered conditions. Each mild steel weld joint was heat treated at 600°C for 1hour and cooled slowly in air at room temperature to stabilize the microstructure and impart the essential mechanical properties.

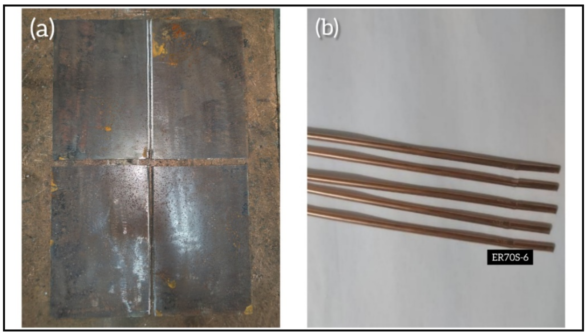

Fig. 1. Materials (a) Base Material (b) Filler Wires.

The different researchers utilize different types of filler metal wire for their experimental study. In this experimental study ER70S6 filler wire is employed having 2.4mm diameter (Khan et al., 2021, Panji et al., 2019) as shown in Fig. 1(b). It composed of iron, in additions with manganese, silicon, and small amounts of other elements, providing good mechanical properties. Commonly used for welding mild steel and is ideal for applications in construction, manufacturing. it has decent resistance to atmospheric corrosion, depending on the environment. This filler wire Shows good toughness, tensile strength and ductility even at lower temperatures, which is essential for many industrial applications.

The chemical composition of base material and filler wire is shown in Table 2.

Table 1. Mechanical property of IS2062E350C.

	Yield strength (MPa)	Tensile strength (MPa)	Elongation (%)
Standard	350 min	410 min	23
After Test	400.30	550.14	38.50

Table 2. Chemical composition of Base material and Filler wire.

Composition	IS2062E350C	Filler wire
C	0.158	0.07
Si	0.0228	0.4-0.7
Mn	1.04	0.9-1.4
P	0.0158	0.025
S	0.0037	0.035
Cr	0.0213	0.0213
Ni	0.0174	0.15
Al	0.05745	-
Cu	0.0097	0.50
W	0.0089	-
Fe	98.6	-

Methodology

Material Preparation

Joining two plates of steel together has become a demanding task in industries for many applications. The dimension 100mm x 150mm of rectangular cross-section were cut from raw sheet using laser cutter as shown in Fig. 2(a). A conventional 'V' groove was made at the edge of the plates, with the groove angle of 60 degree (Elfallah, 2023). Before welding, plates were tacked as shown in Fig. 2(b). Each plate was cleaned using acetone and buffing was also done.

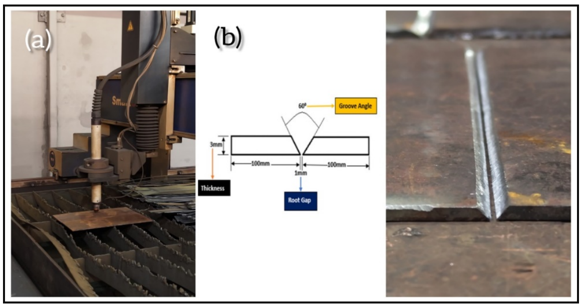

Fig. 2. Sample Preparation for Welding (a) Laser Cutting (b) V-groove Preparation.

Welding Process and Preparation

Before welding, the plates were cleaned with the help of grinder to remove contaminants. The joining process of two plates of mild steel with thickness of 3mm needs proper technique so that joint become defect free and rigid. Welding fixture is used for holding plates for good weld. There are various types of welding are available in the industries. In this research, Gas Tungsten Arc welding (GTAW) have been selected for welding the mild steel plates because of its welding characteristics to weld thin sections. First mild steel plates were tacked at different positions. Two pass 'V' groove butt joints were produced using gas tungsten arc welding (GTAW) machine (Fronius Magic-wave 2200), utilizing 2.4mm diameter ER70S6 filler wire (Panji, 2019). Non-consumable tungsten electrode was used. Welding was performed in the flat position. Welding setup was shown in Fig. 3. The welding process was conducted under optimal conditions, with constant current intensity of 110A maintained throughout entire pass (Singh, 2021, Aninda et al., 2024, Sirohi et al., 2022). Welding was performed in two manually passes, including the backing and capping pass. The welding process parameters for root pass, filling pass, backing pass, and capping pass are listed below in Table 3.

Fig. 3. GTAW Welding Setup.

Table 3. Welding process parameter during welding.

Pass	Current	Voltage	Time
1	110A	9.4V	31sec
2	110A	11.4V	1 min

Post-Weld Heat Treatment (PWHT)

After welding, one set of welded samples was allowed to cool in air (as-welded condition), while another set was subjected to post-weld heat treatment (PWHT) for softening and to reduce brittleness, as depicted in Fig. 4. PWHT is a critical step for components like pressure vessels used in various industries, as it improves corrosion resistance and enhances mechanical performance. In accordance with references (Khan et al., 2021, Dey et al., 2014), the PWHT was carried out at 600 °C for 1 hour. The heating rate was maintained at 10 °C/min, and the samples were furnace-cooled to room temperature at a controlled cooling rate of approximately 5 °C/min to avoid thermal shocks. The entire process was conducted in a muffle furnace under an argon inert gas atmosphere with a flow rate of 2 L/min to prevent oxidation and decarburization of the material surface. After completion of the heat treatment cycle, specimens were extracted from the welded plates for subsequent microstructural examination and mechanical testing to facilitate a comparative analysis between the as-welded and PWHT conditions.

Fig. 4. Post Weld Heat Treatment (PWHT).

Testing Procedure

The welded samples were subjected to various tests, including tensile testing, microhardness testing (Vickers test), and both macrostructure and microstructure analysis. Impact testing was also performed, with each type of test requires specific sample preparation methods. The samples were prepared in accordance with the standards required for each specified test. Test specimens for tensile test was prepared using CNC machine (Wire-EDM) as shown in Fig. 5.


Fig. 5. Wire EDM.

Tensile Test

Tensile test specimens are prepared according to the standards of ASTM E8 (Standard Test Methods for Tension Testing of Metallic Materials) or ISO 6892 (Metallic materials — Tensile testing) as shown in Fig. 6.

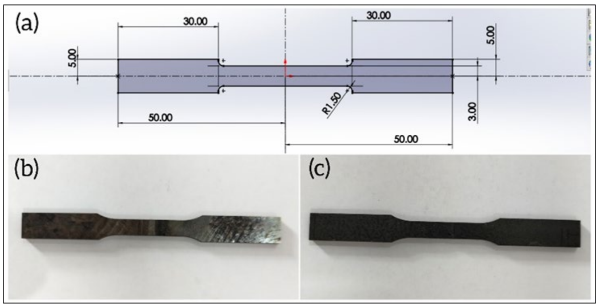

Fig. 6. (a) CAD model (b) Without PWHT Tensile sample (c) PWHT Tensile sample.

These standards outline the dimensions, shape, and preparation methods for the specimens to ensure accurate and reliable test results (Khan et al., 2021). First CAD model of the tensile samples was created by ensuring required dimension and specification described in Fig. 6(a). Then Program the CNC machine (Wire-EDM) with cutting parameters, including feed rate, spark gap, and cutting depth. Test specimen were prepared from both as-welded and PWHT plates as shown in Fig. 6 (b-c). The tensile tests were carried out with the help of universal testing machine (model: UT 10 make ENKAY).

Microhardness Test

Microhardness test was performed to measure distribution of hardness across different phases compositions. Samples of dimensions (26 x 10 mm²) were machined from the welded plate shown in Fig. 7(a, b). The test was conducted with the help of Micro Vickers hardness tester. The hardness was measure at different regions of welded plates before and after of PWHT.

Fig. 7. (a) PWHT Micro-hardness sample (b) Without PWHT Micro-hardness sample.

Impact Test

Impact test was employed to determine the material's resistance to fracture under high stress condition. Charpy V notch test was utilized. The samples were cut according to the standards of ASTM E23. The impact test was employed on standard impact specimen of dimensions (10 x 55 mm²), with V-notch in central to depth of 2mm as shown in Fig. 8(a).

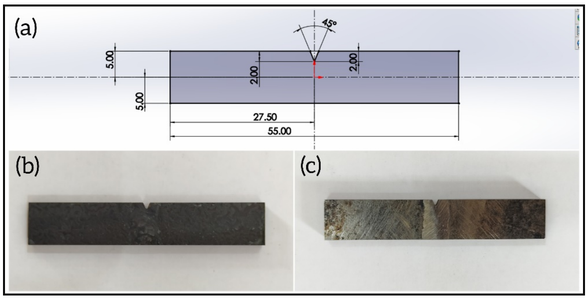

Fig. 8. (a) CAD Model (b) PWHT Impact Sample (c) Without PWHT Impact Sample.

The weld geometry and groove shape proposed by Elfallah (2023). Two samples were prepared from each plate as shown in Fig. 8(b, c). The v-notch was cut in parallel to the welding direction to ensure crack propagation path could pass through backing and capping pass. The test was conducted on Charpy impact tester (Model IT 30 AUTO Impact Tester from FIE).

Macrostructure and Microstructure Analysis

Small rectangular sections (26 x 10 mm²) were cut from as welded joint and as-welded after PWHT sample for microstructure, macrostructure, and microhardness. Careful measurements were taken before cutting sample. samples must cut from weld portion. With the help of wire EDM machine (model E merge S64). The analysis of welded samples involved both macrostructure and microstructure examination. Samples were first cut, polished, and etched to reveal the overall weld structure. Macrostructural analysis was conducted using low-magnification visual inspection to assess weld bead geometry, fusion zones, and visible defects. For microstructural examination, samples underwent fine polishing to a mirror finish, followed by etching to reveal grain boundaries and phases. Optical microscopy was used to examine the microstructure at various magnifications, with particular attention paid to the weld metal, heat-affected zone, and base metal. Grain size measurements and phase identification were performed using standardized techniques.

Sample Size and Reproducibility

To ensure data reliability and reproducibility, all mechanical tests (tensile, impact, and microhardness) were performed on three independently prepared specimens for each condition: base metal, as-welded, and post-weld heat-treated (PWHT). The average of these three values was reported for each test to minimize variability. Care was taken to maintain uniform welding parameters and heat treatment conditions for each set of samples to ensure consistency in the microstructure and mechanical response. The repeatability of results confirms the reliability of the comparative analysis between different weld conditions.

RESULTS AND DISCUSSIONS

Tensile testing, microhardness testing (Vickers test), impact testing, and macrostructure and microstructure analysis were conducted on the prepared samples. For each test, three samples were prepared: one from the base material and two from welded specimens. The results obtained from these tests are presented and discussed in the following sections.

Tensile Test

The welded specimen was post-weld heat treated at 600℃ for 1 hour and tensile tested for comparison with as-welded base metal as shown in Fig. 9(a). The tensile test was performed according to the standards of ASTM E8 by utilizing the Universal Testing Machine (model: UT 10 make ENKAY). All the samples were subjected to axial loading until failure occurred as shown in Fig. 9(b). The specimen after PWHT weld metal showed fracture with a tensile strength of 498.073 MPa and elongation of 23.52%. The tensile strength measure after PWHT welded metal slightly lower tensile strength than the as-welded base metal and elongation in PWHT is 12% more than as-welded base metal as illustrated in Table 4 and Fig. 10. The tensile specimen shows fracture from base metal instead of weld zone, which ensures the joint is safe for the application of a pressure vessel. A decrease in tensile strength was observed after PWHT, which is due to relieving residual stresses that initially enhanced strength, promoting grain growth which reduces resistance to deformation, and redistributing carbon, leading to a softer the weld zone, more ductile microstructure. Post-weld heat treatment (PWHT) at 600°C shows the optimized mechanical properties (Khan et al., 2021, Dey et al., 2014).

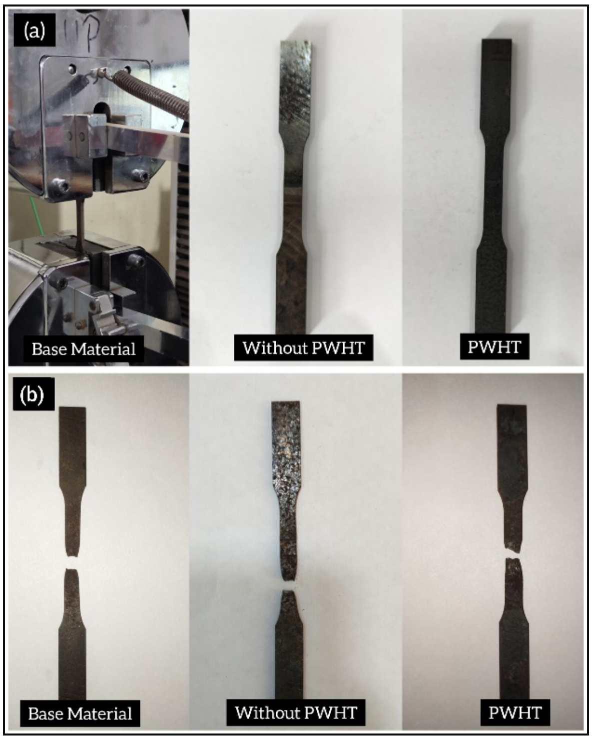

Fig. 9. (a) Samples Before Tensile Test (b) Samples After Tensile Test.

Table 4. Ultimate Tensile Strengths (UTS) of Samples.

SAMPLE / UTS (in MPa)	BASE METAL	PWHT	Without PWHT
TENSILE STRENGTH (MPa)	522.333	498.73	498.74
ELONGATION	33.08%	23.52%	21%

Figure 10 illustrates the ultimate tensile strength (UTS) behavior of the base material, PWHT sample, and the sample without PWHT. Quantitatively, PWHT caused a 4.65% decrease in UTS compared to the base material, which is attributed to stress-relieving and microstructural softening. In contrast, the sample without PWHT showed a 2.53% increase, likely due to strain hardening and formation of harder microstructures, despite potential brittleness. These results reinforce the trade-off between strength and ductility in welded joints depending on post-weld heat treatment application.

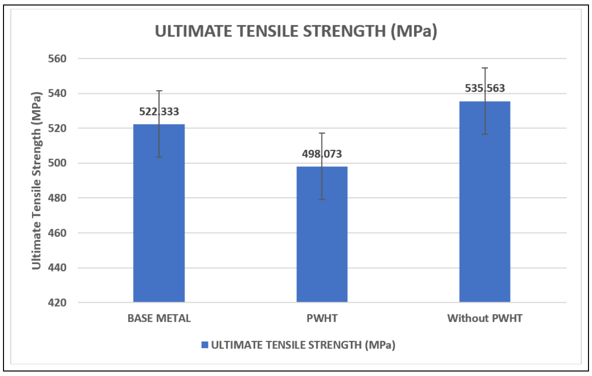

Fig. 10. Graphical representation of Ultimate Tensile Strength (UTS) for base metal, PWHT, and without PWHT samples. Error bars represent ± standard deviation from three independently tested specimens.

Microhardness Test (Vickers Test)

The microhardness profile of the as-welded joint and after PWHT can be seen in Fig. 11(a), the hardness of the weld metal shows the distribution and variation of the harness across three different regions, namely Right Zone (RZ), Weld Zone (WZ), and Left zone (LZ). The method of the Vicker Hardness Test was implemented by utilizing the Micro Vickers Hardness Tester machine (MODEL: MV1-TS) as shown in Fig. 11(b). As can be seen, PWHT for 1 hour at 600 °C had a significant effect on the hardness of HAZ and weld metal, decreasing severely. This reduction in hardness becomes much more evident in the weld metal. This significant decrease is primarily due to the relief of residual stresses in the weld zone (Bhanu et al., 2022). PWHT allows the material to undergo stress relaxation and, the formation of coarse grains which reduces the dislocations and internal stresses caused by the welding process, thereby lowering the hardness in the weld metal and making the material less brittle (Kaur et al., 2014). The microhardness results reveal that post-weld heat treatment (PWHT) led to a reduction in hardness across all zones, with the welded zone (WZ) showing a 14.89% decrease compared to the base material. Conversely, the sample without PWHT exhibited substantial hardening, with WZ reaching a peak increase of 41.59%, likely due to untempered martensite formation. This quantification highlights the importance of PWHT in controlling hardness variations and potential brittleness in welded joints. Here is a summarized Table 5 and Fig.12 with standard results showing the hardness values of different zones of the weld joint in both the as-welded condition and post-weld heat treatment (PWHT) conditions.

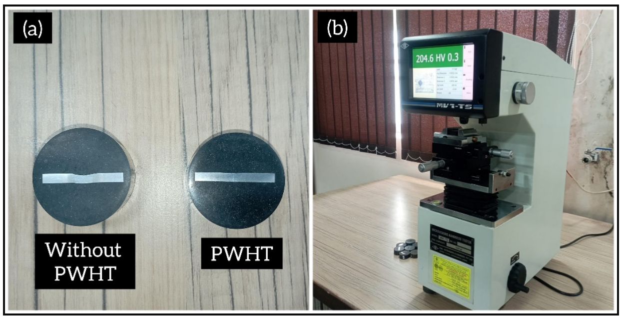

Fig. 11. (a) Samples for Micro-hardness Test (b) Vickers Hardness Testing Machine.

Table 5. Vickers Microhardness values of samples.

SAMPLE / ZONE	Base Metal	Without PWHT	PWHT
Right Zone (RZ)	179.33 HV	213.86 HV	157.96 HV
Weld Zone (WZ)	179.33 HV	254.00 HV	152.60 HV
Left Zone (LZ)	179.33 HV	185.36 HV	160.23 HV

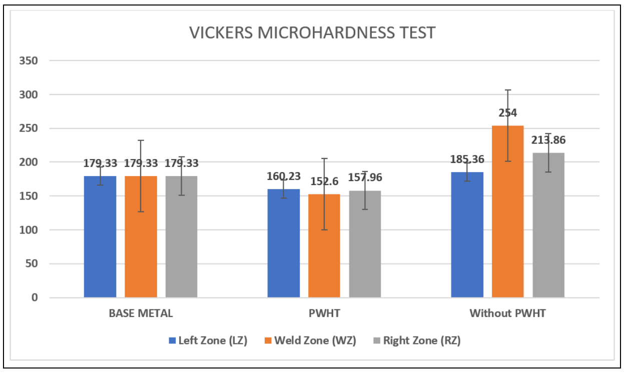

Fig. 12. Graphical representation of Vickers Hardness test for base metal, PWHT, and without PWHT samples. Error bars represent ± standard deviation from three independently tested specimens.

Impact Test

To meet the crucial requirement for testing the vessel, the minimum impact toughness required for the grade IS20062E350C is 27 J. The Charpy V-notch impact toughness test was employed in order to determine the toughness of the samples. The impact specimen before and after fracture is shown in the Fig. 13(a-b). The impact toughness of the welded joint is 33J. The fracture specimen of the as-welded joint supports the impact toughness test as it breaks into two parts. The impact toughness test after PWHT can be affected by the specific heat treatment process, including the temperature, time, and cooling rate. The average absorbed energy results of as-welded base metal and after PWHT weld metal are shown in the Fig. 14. The highest impact toughness of 42.5J is absorbed in the sample after PWHT, while the lowest impact toughness of 33J is absorbed in the as-welded base metal sample which is described in Table 6. Toughness is increased by the PWHT. PWHT for 1 hour significantly increases the weld toughness due to tempering and softening of metal (Khan et al., 2021, Dey et al., 2014). The test was conducted on Charpy impact tester (Model IT 30 AUTO Impact Tester from FIE).

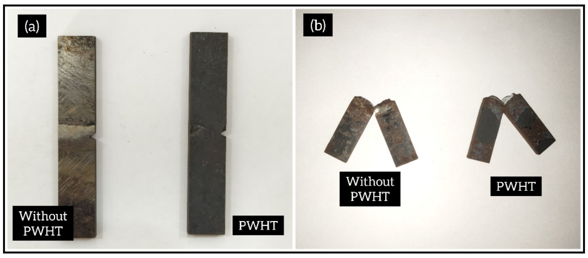

Fig. 13. (a) Impact Samples Before Test (b) Impact Samples After Test.

Table 6. Absorbed impact energy of samples.

Sample No.	Material	Absorbed Impact Energy (J)
1	Base Metal	34
2	PWHT	42.5
3	Without PWHT	33

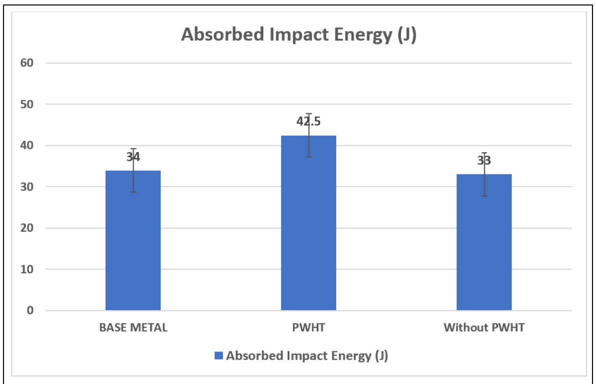

Fig. 14. Graphical representation of Absorbed Impact Energy for base metal, PWHT, and without PWHT samples. Error bars represent ± standard deviation from three independently tested specimens.

As shown in Figure 14, the absorbed energy of the PWHT sample increased by 25% over the base metal, confirming the improved impact toughness due to stress relief and refined grain structure. In contrast, the sample without PWHT showed a marginal 2.94% decrease in impact energy, suggesting reduced ductility and higher brittleness. These findings align with the hardness trends and underscore the role of PWHT in enhancing the toughness of welded joints.

Macrostructure Analysis

Here is a focused analysis comparing two welded samples: one with post-weld heat treatment (PWHT) and one without PWHT. This approach will reveal how PWHT affects structural integrity, Heat affected Zone (HAZ) properties, and defect formation in Fusion Zone (FZ).

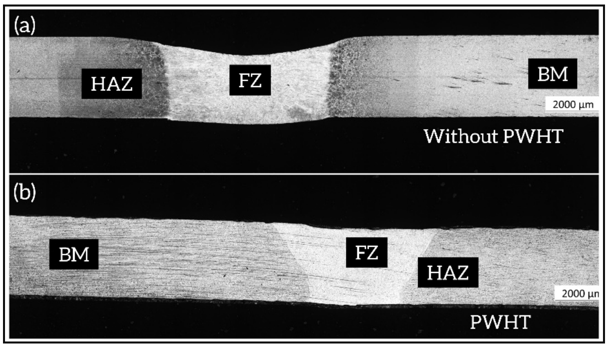

Fig. 15. Macrostructure Images of Welded Samples (a) Without PWHT (b) PWHT.

The Without PWHT sample exhibited broader, less uniform grain structures in the HAZ as shown in Fig. 15(a) due to rapid cooling, leading to residual stresses, grain coarsening, and a higher likelihood of defects such as micro-cracks or undercuts. These attributes can reduce ductility and increase susceptibility to brittle fractures, compromising the material's overall toughness and performance under stress.

In contrast, PWHT significantly improved the uniformity and homogeneity of the welded structure by refining grains, relieving residual stresses, and enhancing weld bead cohesion. The PWHT sample exhibited a more stable HAZ as shown in Fig. 15(b) with fewer discontinuities, leading to balanced hardness, enhanced ductility, and improved toughness across the weldment. This uniformity strengthens the material's resilience and reduces the likelihood of stress-related failures.

Ultimately, implementing PWHT is essential for welded structures requiring high reliability and durability, as it stabilizes the microstructure and enhances the mechanical properties of the weld and surrounding base metal.

Microstructure Analysis

The microstructure analysis of the base material (IS2062E350C) and various welded samples has provided valuable insights into the effects of PWHT. The distinct zones—Base Metal (BM), Fusion Zone (FZ), and Heat Affected Zone (HAZ)—display variations in their microstructural properties, which are crucial for understanding the mechanical performance of the welded joints.

Fig. 16 shows that the base material,

IS2062E350C steel, primarily consists of ferrite and pearlite. The fine-grained structure observed in Fig.16(b) suggests a balanced combination of strength and ductility. The grains appear more uniform and rounded compared to the as-welded sample. This is characteristic of a stress-relief annealing process. The coarser grains suggest recrystallization and grain growth at 600°C, which reduces the hardness but improves toughness and ductility (Gharibshahiyan et al., 2011). The microstructure displays sharp, needle-like patterns as reflected in Fig. 16(a) of martensitic or bainitic phases, indicating high hardness and tensile strength but reduced ductility due to rapid cooling.

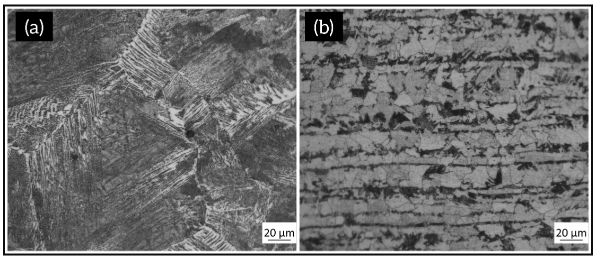

Fig. 16. Microstructure of Base Material Zone (a) Without PWHT (b) PWHT.

Fig. 17 shows microstructure of PWHT sample, in this case, the FZ exhibits a mix of Pearlite and Ferritic phases. PWHT reduces grain coarsening in the HAZ by promoting a more uniform grain structure, thereby enhancing ductility and toughness. This reduction in grain size improves the material's ability to withstand stress without fracturing, which is essential in high-stress applications.

The slow cooling of PWHT relieves residual stresses in the FZ and HAZ, which minimizes susceptibility to cracking. Furthermore, this process can stabilize the microstructure by inducing phase transformations that make the joint more resilient. The tempered microstructure achieved through PWHT strikes a balance between hardness and toughness (Dey et al., 2014). The presence of the HAZ near the weld interface is evident, with noticeable reduction in grain coarsening Fig. 17(a, b). This reduction in grain growth in the HAZ brittleness may decrease, affecting the weld's mechanical integrity.

The without PWHT sample retains significant hardness, attributed to rapid cooling rates following the welding process. This cooling creates a dendritic structure in the Fusion Zone (FZ) and a coarse-grained structure in the Heat Affected Zone (HAZ) as shown in Fig. 18(c, d).

The coarse-grained microstructure within the HAZ Fig. 18(c), resulting from high thermal gradients, decreases the material's ability to absorb energy under impact. As shown in Fig.18(a, b) ferrite appears as lighter-coloured regions which is relatively soft and ductile phase in steel. Fine ferrite grains are smaller in size, which enhance the material's strength due to grain boundary strengthening (Hall-Petch relationship). Pearlite appears as darker regions which is lamellar structure composed of alternating layer of ferrite and cementite. Their formation is takes place due to controlled cooling rate during heat treatments such as normalizing.

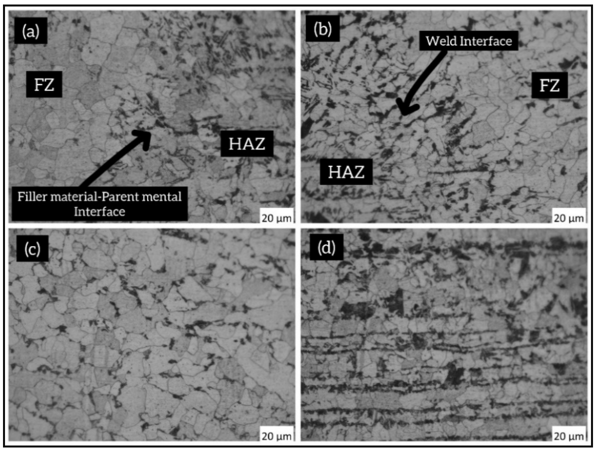

Fig. 17. Microstructure of PWHT Sample (a) showing HAZ, FZ, weld interface of left portion at 20µm (b) HAZ and FZ at 20µm (c) FZ at 20µm (d) HAZ at 20µm.

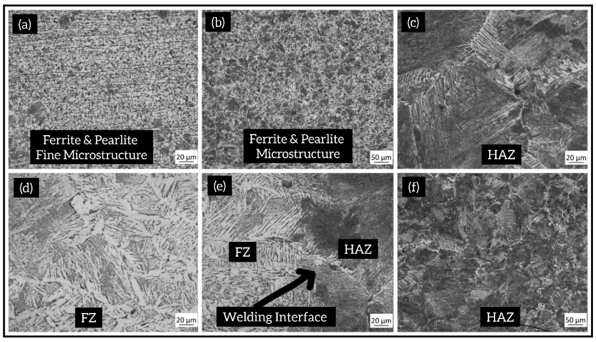

Fig. 18. Microstructure of Without PWHT Sample (a)Base Material at 20µm (b) Base Material at 50µm (c)HAZ at 20µm (d)FZ at 20µm (e)Welding Interface at 20µm (f)HAZ at 50µm.

In Fig.18(e) shows the weld metal and parent metal interface which is a critical region in a welded joint, often referred to as the fusion line. It marks the boundary where the weld metal solidifies and bonds with the base metal. Fig.18(f) depicts low carbon martensite with ferrite at grain boundaries, that indicates dual phase structure provides an optimal balance of strength and toughness. Low carbon martensite contributes to high strength and hardness. While the ferrite phase at the grain boundaries enhances ductility and impact resistance. Cooling that occurs without PWHT leaves residual stresses in the FZ and HAZ. These stresses, if not alleviated, may reduce fatigue resistance, and increase the likelihood of crack initiation.

Quantitative microstructural analysis was performed using ImageJ software to evaluate the average grain size and phase fraction in different zones of the weldment, including the Base Metal (BM), Fusion Zone (FZ), and Heat-Affected Zone (HAZ). The average grain size was measured using the intercept method on multiple micrographs captured at 200× and 500× magnifications. The analysis revealed that the base metal exhibited an average grain size of approximately 11.4 µm. In the fusion zone, the grain size was significantly coarser in the sample without post-weld heat treatment (PWHT), measuring around 19.2 µm, whereas the PWHT-treated fusion zone showed refined grains with an average size of about 13.5 µm. Similarly, in the HAZ, the grain size was approximately 16.8 µm without PWHT and was reduced to 12.2 µm following PWHT. Phase fraction analysis was also conducted by thresholding grayscale images to quantify the relative area of constituent phases. In the PWHT-treated fusion zone, the ferrite phase occupied roughly 74% of the area, while the harder pearlite or martensite phases constituted around 26%. This shift in phase distribution indicates a reduction in brittle microstructures and a corresponding enhancement in ductility and impact toughness due to PWHT. These quantified observations support the qualitative findings of improved mechanical performance and microstructural stability in PWHT-treated samples.

CONCLUSIONS AND FUTURE SCOPE OF WORK

This study provides a comprehensive assessment of the influence of post-weld heat treatment (PWHT) on the microstructure and mechanical properties of GTAW-welded IS2062E350C mild steel, used in pressure vessel applications. Based on experimental observations and analysis, the following key findings were derived:

- PWHT significantly enhanced impact toughness, with the absorbed energy increasing from 33 J to 42.5 J, improving the joint's fracture resistance.
- The hardness in the weld and heat-affected zones decreased after PWHT, with the weld zone showing a 14.89% reduction, indicating better ductility and stress relief.
- Tensile strength reduced slightly post-PWHT (from 535.563 MPa to 498.073 MPa), yet remained above the minimum required for structural integrity in pressure vessels.
- Elongation improved in PWHT samples, rising from 21% to 23.52%, signifying enhanced plastic deformation capacity.
- Microstructural analysis showed grain refinement in the fusion and heat-affected zones after PWHT, with average grain size reducing significantly compared to as-welded joints.
- PWHT altered the phase composition in the fusion zone, increasing the ferrite fraction to approximately 74%, contributing to reduced brittleness.
- Macrostructural examination confirmed improved weld bead uniformity and reduced defect formation in PWHT samples.

These findings demonstrate that PWHT at 600 °C for 1 hour is effective in achieving a desirable balance between strength, toughness, and ductility. The results support the application of PWHT to improve the reliability and service life of pressure vessel components in critical industries such as oil and gas, chemical processing, and power generation.

Further studies can explore the long-term performance of PWHT-treated welds under fatigue, creep, and cyclic loads. Optimization of PWHT parameters, comparison with other welding methods, corrosion behavior in harsh environments, and simulation-based modeling of residual stresses can enhance understanding and broaden industrial applications.

REFERENCES

Ahmed, Y.M., Hameed D.L., and Azhin A.A, "Study the durability of welding and performance of base metal of LPG home cylindrical manufactured in Kurdistan region," *Journal of Energy, Mechanical, Material, and Manufacturing Engineering* 4, no. 2: 91-100 (2019).

Aninda, R.K., Shazrina M.K., Redwan S., Md, M.R., and Md, I.I.R, "Effect of post-weld heat treatment on mechanical properties and microstructure in electric arc welded mild steel joints," *Journal of Engineering Research* 12, no. 2: 210-215 (2024).

Bhanu, V., Shailesh, M.P., Gupta A., and Pandey, C, "Dissimilar weldments of P91 and Incoloy 800HT: Microstructure, mechanical properties, and residual stresses," *International Journal of Pressure Vessels and Piping* 199: 104782 (2022).

Boumerzoug, Z., Chemseddine D., and Thierry, B, "Effect of welding on microstructure and mechanical properties of an industrial low carbon steel," *Engineering* 2, no. 7: 502 (2010).

Dey, H.C., Albert, S.K., Bhaduri, A.K., Roy, G.G., Balakrishnan, R., and Panneerselvi, S, "Effect of post-weld heat treatment (PWHT) time and multiple PWHT on mechanical properties of multi-pass TIG weld joints of modified 9Cr-1Mo steel," *Welding in the World* 58: 389-395 (2014).

Elfallah, S, "Influence of Groove shape on the Mechanical Properties of Welded Commercial Steel," *Welding Technology*

Review 95 (2023).

Gharibshahiyan, E., Abbas H.R., Nader P., and Mehdi R, "The effect of microstructure on hardness and toughness of low carbon welded steel using inert gas welding," *Materials & Design* 32, no. 4: 2042-2048 (2011).

Kaur, G., Singh, D., and Jasmaninder S.G, "Effect of filler wire composition on joining properties of GTAW stainless steel 202," In *Proceedings of the International Conference on Research and Innovations in Mechanical Engineering: ICRIME-2013*, pp. 191-200. New Delhi: Springer India (2014).

Khan, M., Mohammad W.D., and Md, Z.S, "Effects of welding technique, filler metal and post-weld heat treatment on stainless steel and mild steel dissimilar welding joint," *Journal of Manufacturing Processes* 64: 1307-1321 (2021).

Kumar, S., Chandan, P., and Amit, G, "Effect of post-weld heat treatment and dissimilar filler metal composition on the microstructural developments, and mechanical properties of gas tungsten arc welded joint of P91 steel," *International Journal of Pressure Vessels and Piping* 191: 104373 (2021).

Nilsen, K, "Development of low-pressure filter testing vessel and analysis of electrospun nanofiber membranes for water treatment," *PhD diss., Wichita State University, College of Engineering, Department of Mechanical Engineering* (2011).

Panji, M., Baskoro, A.S., and Widyianto, A., "Effect of welding current and welding speed on weld geometry and distortion in TIG welding of A36 mild steel pipe with V-groove joint," In *IOP Conference Series: Materials Science and Engineering*, vol. 694, no. 1, p. 012026. IOP Publishing (2019).

Sadeghi, B., Hassan, S., Mahdi, R., and Morteza T, "Effects of post weld heat treatment on residual stress and mechanical properties of GTAW: The case of joining A537CL1 pressure vessel steel and A321 austenitic stainless steel," *Engineering Failure Analysis* 94: 396-406 (2018).

Singh, G, "A review on effect of heat treatment on the properties of mild steel," *Materials Today: Proceedings* 37: 2266-2268 (2021).

Sirohi, S., Amit, K., Shiva, S., Gaurav, D., Sanjeev, K., Aleksandra, Ś., Grzegorz, R., Dariusz, F., and Chandan, P, "Influence of PWHT parameters on the mechanical properties and microstructural behavior of multi-pass GTAW joints of P92 steel," *Materials* 15, no. 12: 4045 (2022).

Toudehdehghan, A., and Tan, W.H, "A critical review and analysis of pressure vessel structures," In *IOP Conference series: materials science and engineering*, vol. 469, no. 1, p. 012009. IOP Publishing (2019).